Activity report of the Italian CRG beamline at the European Synchrotron Radiation Facility (ESRF)

N. 9 - January 2022

Grenoble, January 2022

Responsabile editoriale: Francesco d'Acapito
(*dacapito@iom.cnr.it*)

Editing: Roberta De Donatis
(*roberta.dedonatis@cnr.it*)

ISSN 2553-9248

LISA

Annual Report 2021

ISTITUTO OFFICINA DEI MATERIALI

Abstract

This document resumes the activity of the Italian CRG beamline at ESRF (LISA project) during year 2021. The latest news from the beamline are presented as well as details on the technical activity, highlight experiments and publications.

Keywords

Italian beamline at ESRF, BM08

LISA project

X-ray Absorption Spectroscopy

Index

1. Foreword

2021 has been the first year of full activity for LISA with the new instrumentation and the new EBS source. Some limitations have been encountered due to the partial lockdown / travel restrictions in the first part of the year so a few experiments had to be carried out in 'mail in' mode. Full activity in presence could be recovered starting from run3 (May). During year 2021 LISA has carried out 21 experiments (10 ESRF and 21 CRG) for a total amount of 348 shifts (171 ESRF, 177 CRG). The CRG users have benefited from the financial support of CERIC-ERIC. Concerning publications this year has been particularly depleted due to the conjuncture of the refurbishment of the beamline, the long shutdown of ESRF and the subsequent pandemic crisis. However, the intense activity observed in 2021 makes us confident of a restart of a richer crop next year.

Some technical advancements on the beamline have been carried out namely the setup of a facility of X-ray Powder diffraction station and a feedthrough flange making possible the use of the microtomo cell in a He environment.

On the personnel side we all owe a warm goodbye to Alessandro Puri who has terminated his contract at LISA last April. Concerning visitors LISA in2021 LISA has hosted for 3 weeks Sara Laureti from CNR-ISM-Montelibretti in the framework of a project on magnetic alloys and two students Tommaso Baroni and Alessio d'Acapito (respectively from Florence and Grenoble universities) who helped running the beamline during this year and contributed to the development of some data collection methods. New post Docs has been hired: Abdul Rehman Malik and Michela Brunelli and they will be operative in 2022.

2.1. Glove box

A 2 places glovebox (model PLAS-LABS - #855 ACB) has been installed in the sample preparation laboratory and it is shown in Figure 1:

Figure 1. Left: Overview of the 2-places glove box. Right: detail of the transfer chamber.

2.2. Feedthrough flange for the microtomo cell

Since a few years the MICROTOMO cell is available at LISA for carrying out experiments at high temperature and controlled atmosphere. The setup is highly efficient but up to now the experiments were carried out in air due to the presence of electrical and fluid connections between the MICROTOMO cell and its control unit. In collaboration with the sample environment group of ESRF a flange with all the needed feedthroughs has been realized so that the cell can be closed in the measurement chamber and placed under helium atmosphere. A gain of up a factor 10 in intensity on the I1 chamber (after the sample) has been reported in the energy range 5-7 keV so leading to the collection of data of increased quality.

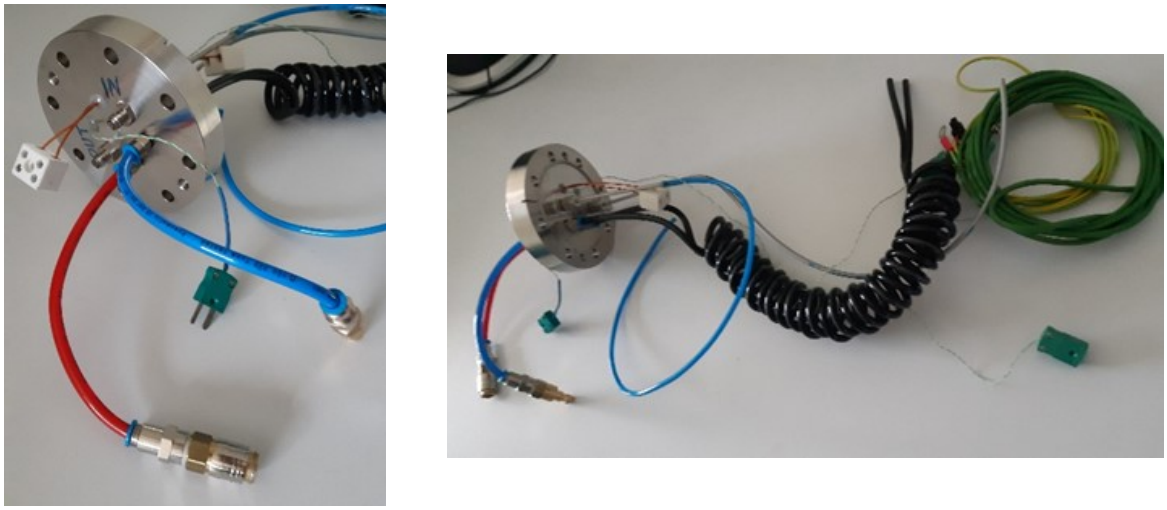

Figure 2. Left: detail of the 'user' side of the feedthrough flange with the connection for the cooling water, treatment gas, thermocouple and heater supply. Right: view of the 'cell' side.

2.3. X-ray powder diffraction facility

An X-ray powder diffraction (XRPD) end-station has been recently installed on LISA (Figure 4, left). The end-station is positioned in the experimental hutch 2, downstream the vacuum EXAFS chamber and it essentially consists of a spinner motor equipped with a holder for standard goniometric heads where capillaries can be mounted. The spinner is held on a support providing vertical and horizontal alignment of the sample. A MAR 165 CCD detector is placed at about 30 cm from the capillary.

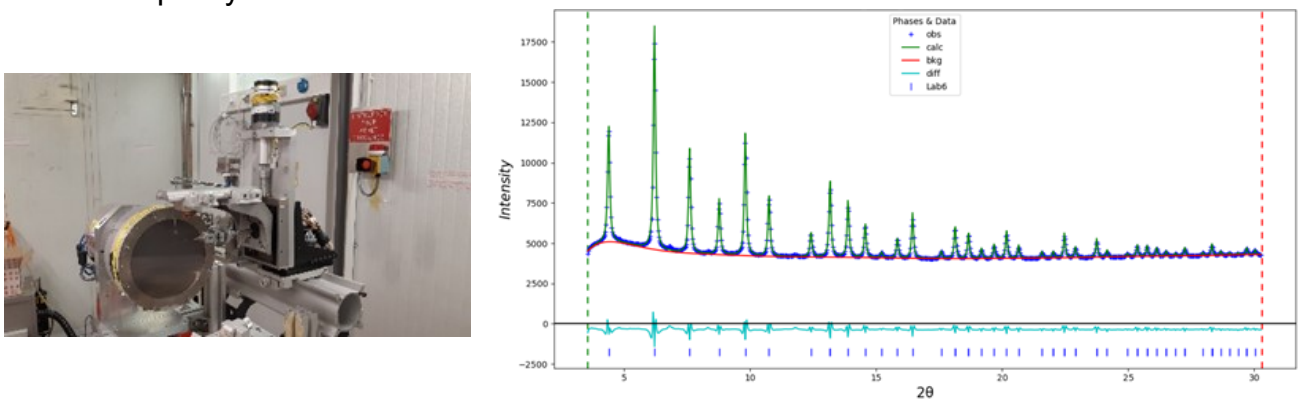

Figure 4. Upper left) Picture of the XRD experimental setup in LISA experimental hutch; right) Rietveld refinement with X-ray diffraction pattern of LaB6 measured with the 2D MAR165 CCD detector

Here we report XRPD tests performed at 39 KeV (λ=0.3179 Å) on a NIST LaB_6 powder (S.G. $Pm\bar{3}m$; a = 4.1568 Å) loaded into a 0.5 mm diameter capillary; energy was calibrated using Ce K edge (40.443 KeV) as a reference; beam size on sample was ~80 (h)*120 (v) μm^2 (Figure 4, right). Detector distance, rotation and tilting angles were calibrated with the FIT2D package [1] employing the diffraction pattern measured on Cr_2O_3 powder as a reference. The 2D Debye-Scherrer circles were registered as 2D raw frames, and processed into 1D powder patterns using FIT 2D software (Figure 4, bottom; acquisition time 300 s). Rietveld refinement on collected data was performed up to d = 0.61 Å (R_w= 1.940%) using GSAS II package [2]. The refined unit cell parameter [a = 4.161 Å] agrees with the reference values within 0.005 Å.

More diffraction tests will be performed on LISA in the near future in order to improve the current setup and fully assess the potentiality of the beamline for X-ray diffraction. All in all, the preliminary results here briefly reported prove the feasibility of diffraction experiments on LISA. The availability of a XRPD end-station allows LISA users to couple local atomic information obtained by X-ray absorption spectroscopy measurements, the standard technique on BM08, with average long-range structural data on the studied phases. The simple geometry of the XRPD experimental setup allows, in principle, the simultaneous collection of XAS and XRPD data. Likewise, non-standard sample environments such as low/high-temperature using a cryogun or a gas blower could also be implemented.

[1] Hammersley, A. P. (2016). FIT2D: a multi-purpose data reduction, analysis and visualization program. Journal of Applied Crystallography, 49(2), 646-652.

[2] Toby, B. H., & Von Dreele, R. B. (2013). GSAS-II: the genesis of a modern open-source all purpose crystallography software package. Journal of Applied Crystallography, 46(2), 544-549.

2.4. XAS on biological samples

A major problem in collecting XAS data on radiation-sensitive biological samples in acqueous solution is that they need to be frozen to minimize radiation damage while avoiding the formation of crystalline ice. In addition to this we have to take into account that the amount of sample typically available is limited to a few tens μl. We have successfully tested the use of small kapton tubes of 1mm diameter in our 'cool chamber' cryostat (Figure 3, left) for the collection of XAS data on metalloproteins. The tube was cut at a length of approx. 3cm and mounted on the sample holder (Figure 4, right). The loading was performed using the "bird feeding technique": the liquid sample is loaded using a 0.5-10μL pipette and transferred to the Kapton tube drop by drop by light pressure on the pipette piston. The drops are absorbed in the tube by capillarity. The volume loaded for the experiments can range between 1 and 10 μL.

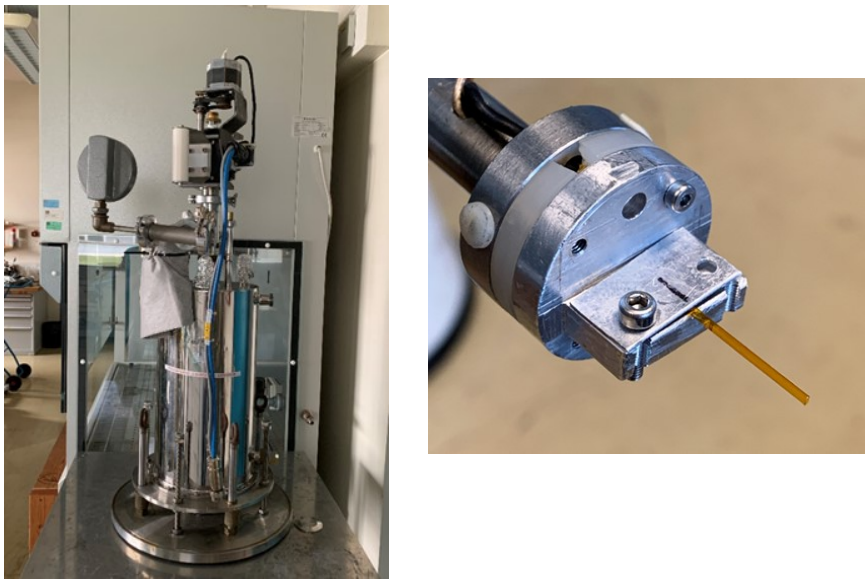

Figure 5. Apparatus for data collection on biological samples. Left: the 'cool chamber' Liquid Nitrogen cryostat. Right: The Kapton tube on the sample holder

Successively, the sample was plunge-frozen in liquid nitrogen (in a beaker placed next to the chamber) for 30 seconds and immediately transferred into the cryostat chamber and kept at about 100 K. The good quality of the XAS data collected (see Figure 5) demonstrate the effectiveness of the method.

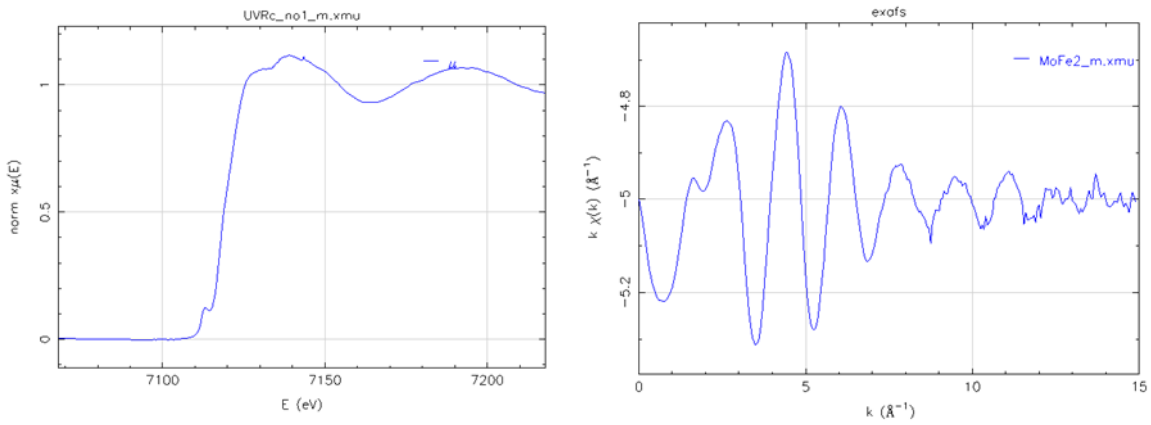

Figure 6. XAS data collected at the Fe-K edge at 100K in the kapton tube on a metalloprotein concentrated at 1Mmol. Left: XANES region, right EXAFS signal.

3.1.

Copper oxide nanomaterial fate in plant tissue: Nanoscale impacts on reproductive tissues

M. Marmiroli,[1,] L. Pagano,[1,*] R. Rossi,[1] R. De La Torre-Roche,[2] G. O. Lepore,[3] R. Ruotolo,[1] G. Gariani,[4] V. Bonanni,[4] S. Pollastri,[4] A. Puri,[5] A. Gianoncelli,[4] G. Aquilanti,[4] F. d'Acapito,[5] J. C. White,[2,§] N. Marmiroli[1,6,§,#]*

[1] Department of Chemistry, Life Sciences and Environmental Sustainability, University of Parma, Parco Area delle Scienze 11/A, 43124 Parma, Italy. [2] The Connecticut Agricultural Experiment Station, 123 Huntington Street, 06504 New Haven, CT, USA. [3] Earth Science Department, Univeristy of Florence, Via La Pira 4, 50121 Firenze, Italy. [4] Elettra, Sincrotrone Trieste, Strada Statale 14 - km 163,5 in AREA Science Park, 34149 Trieste, Italy. [5] CNR-IOM-OGG c/o ESRF – The European Synchrotron, 71 Avenue des Martyrs CS 40220, F-38043 Grenoble Cédex 9, France. 6 Consorzio Interuniversitario Nazionale per le Scienze Ambientali (CINSA), University of Parma, 43124 Parma, Italy.

A thorough understanding of the implications of chronic low dose exposure to Engineered Nanomaterials (ENMs) through the food chain is lacking. The present study aimed to characterize such response in *Cucurbita pepo* L. (zucchini) upon exposure to a potential nanoscale fertilizer: copper oxide (CuO) nanoparticles. Zucchini was grown in soil amended with nano-CuO, bulk CuO (100 mg Kg^{-1}) and $CuSO_4$ (320 mg Kg^{-1}) from germination to flowering (60 days). Nano-CuO treatment had no impact on plant morphology or growth, nor pollen formation and viability. The uptake of Cu was comparable in the plant tissues under all treatments. RNA-seq analyses on vegetative and reproductive tissues highlighted common and nanoscale-specific component of the response. Mitochondrial and chloroplast functions were uniquely modulated in response to nanomaterial exposure as compared with conventional bulk and salt forms. X-ray Absorption Spectroscopy (XAS) performed at BM08 "LISA" beamline (ESRF, France). XAS measurements at the Cu K-edge (8978.9 eV) were performed using plant samples and three model compounds: CuO (bulk), CuO NPs and $CuSO_4 \cdot 5H_2O$. The main optical features of the beamline were a fixed exit monochromator with a pair of Si (111) crystals (energy resolution $\Delta E/E \approx 1.33 \cdot 10^{-4}$); Si mirrors were used for harmonics rejection (E cutoff ≈ 15 KeV). Energy was calibrated with a Cu reference foil (8978.9 eV). In order to minimize beam-induced damage, spectra of samples were acquired at 80 K with a constant k step of 0.05 $Å^{-1}$ up to a maximum k value of 12.5 $Å^{-1}$ for plant tissues while model compounds were measured at room temperature with a k step of 0.03 $Å^{-1}$ up to k=18 $Å^{-1}$. Plant samples were measured in the fluorescence mode with a 12-element HP-Ge detector while model compounds were measured in transmission mode. EXAFS spectra were fitted through the ARTEMIS software in the Fourier-Transform (FT) space. The XAS analyses showed that Cu local structure changed upon nano-CuO internalization, suggesting potential nanoparticles biotransformation within the plant tissues. These findings demonstrate the potential positive physiological, cellular, and molecular response related to nano-CuO application as a plant fertilizer, highlighting the differential mechanisms involved in the exposure to Cu in nanoscale, bulk or salt forms. Nano-CuO uniquely stimulates plant response in a way that can minimize agrochemical inputs to the environment, and therefore could be an important strategy in nano-enabled agriculture.

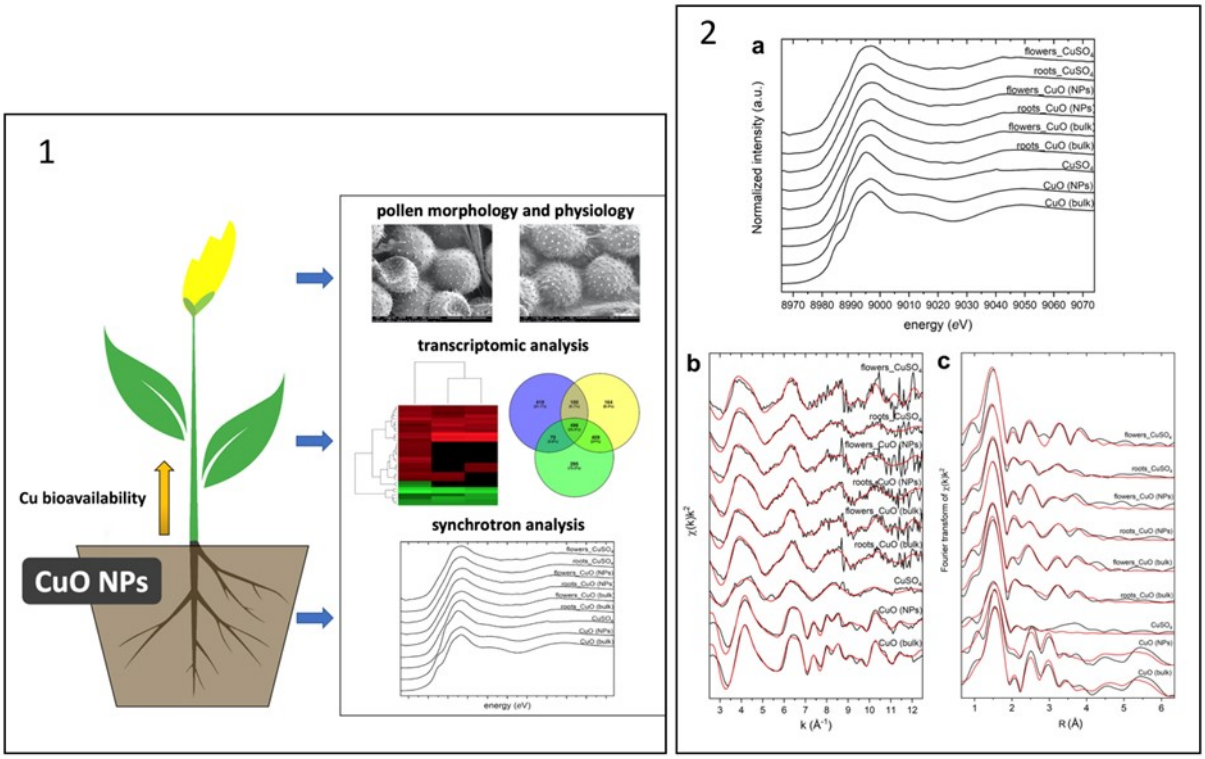

Figure 7: Experimental design with the treatments and the different pollen analyses. 2) XANES spectra of the measured samples and model compounds (a). Cu K-edge k^2-weighted EXAFS region (b) and Fourier transforms (c) of plant tissues and model compounds. Solid lines are data, red lines are fits. Energy was calibrated with a Cu reference foil (8978.9 eV). In order to minimize beam-induced damage, spectra of samples were acquired at 80 K with a constant k step of 0.05 $Å^{-1}$ up to a maximum k value of 12.5 $Å^{-1}$ for plant tissues while model compounds were measured at room temperature with a k step of 0.03 $Å^{-1}$ up to k=18 $Å^{-1}$. Plant samples were measured in the fluorescence mode with a 12-element HP-Ge detector.

Publication: Marmiroli M. et al. - Environmental Science and Technology 55, 10769-10783, (2021)

Iron- and cobalt-doped ZnO lithium-ion battery anodes: An investigation of the (de-) lithiation reaction mechanism by X-ray absorption spectroscopy

A. Trapananti[1], T. Eisenmann[2,3] ,G. Giuli[1] , F. Mueller[2,3], A. Moretti[2,3], S. Passerini[2,3], and D. Bresser[2,3]

[1]University of Camerino, [2]Helmholtz Institute Ulm (HIU), [3]Karlsruhe Institute of Technology (KIT)

Lithium-ion batteries (LIBs) are the state-of-the art electrochemical energy storage technology and the continuously increasing demand calls for intensified research to develop devices that are characterized by enhanced and application-tailored performances, lower cost as well as greater safety and environmental friendliness [1]. This concerns in particular the development of novel electrode active materials.

With regard to the anode, simple metal oxides such as ZnO or SnO_2 have emerged as possible alternatives to the commercially used graphite. Nonetheless such materials suffer of rapid capacity fading which limits the potential for their application. In recent studies, it was found that doping ZnO with transition metals (TMs) such as Fe or Co allows for long-term stable cycling of such materials at specific capacities equivalent or close to the theoretical maximum of about 1000 mAh g^{-1} [2]. Although the general reaction mechanism was investigated by *operando* X-ray diffraction, some aspects of the conversion-alloying reaction by which lithium is stored in such materials remained to be clarified, notably the impact of the chemical nature of the dopant and its initial oxidation state. Synchrotron-based X-ray absorption spectroscopy (XAS) is particularly well suited for developing a deeper understanding of transition metal oxide compounds in LIBs, especially when amorphous or nanocrystalline phases are involved.

An in-depth XAS investigation of (carbon-coated) Fe- and Co-doped ZnO anodes was therefore performed at beamline LISA-BM08 of the ESRF. XAS spectra were measured both *ex situ* and *operando* along the first discharge (lithiation) and charge (de-lithiation). In a previous studies of the pristine materials, both dopants were found to substitute Zn in the wurtzite crystal structure, with the inserted iron being almost purely (95%) trivalent while cobalt is purely divalent [3]. For both materials, XAS spectra were collected on anodes recovered at selected potentials along the first dis-/charge cycle. The expected reduction of Zn^{2+} to metallic Zn is clearly shown by the edge shift towards lower energy (Figure 7 a,b - left). Moreover, the edge position of the two fully lithiated electrodes (at 0.01 V) is further shifted to lower values than for Zn metal, which indicates the eventual formation of the Li_xZn alloy. Spectral features of the oxide phase are again evident in the spectra collected in the fully charged state, revealing that a large fraction of Zn is re-oxidized to Zn^{2+}. The metallic and oxide fractions along the lithiation/de-lithiation reaction, as determined by linear combination fitting analysis of the Zn K-edge XANES spectra, are shown in Figure 7 c,d.

At the end of the first cycle, the fraction of re-oxidized zinc is almost 80% for both Fe and Co dopants, a fraction substantially higher than what has been reported for pure ZnO [4]. The metal doping is therefore favoring the reversibility of the conversion reaction and the re-oxidized fraction is almost independent of the chemical nature and oxidation state of the dopant.

The analysis of the EXAFS signals (Figure 7 right a,b) further elucidates the nature of the metallic phases formed upon lithiation. For the fully lithiated materials, highly damped single-shell EXAFS signals of metallic Fe and Co phases were recorded and the quantitative analysis indicates the formation of very small (few nm) and/or highly defective metallic nanoclusters. The initial oxidation state of the dopant affects the initial reduction kinetics, with the Fe (and also Zn) reduction occurring at significantly higher potentials (Figure 7), at least partially owing to the initial Li^+ insertion favored by vacancies associated with the aliovalent doping [3].

The overall results of this work provide fundamental insights into the mechanism of the conversion-alloying reaction taking place in Fe- and Co-doped ZnO anodes. The TM doping results for both dopants in a greatly increased re-oxidation of zinc compared to pure zinc oxide and, thus, a substantially higher reversible capacity. The choice of the dopant and its initial oxidation state, isovalent (Co^{2+}) or aliovalent (Fe^{3+}) in ZnO affects the lithiation kinetics. These findings may help to develop further advanced active materials for LIBs based on metal oxides and alloys.

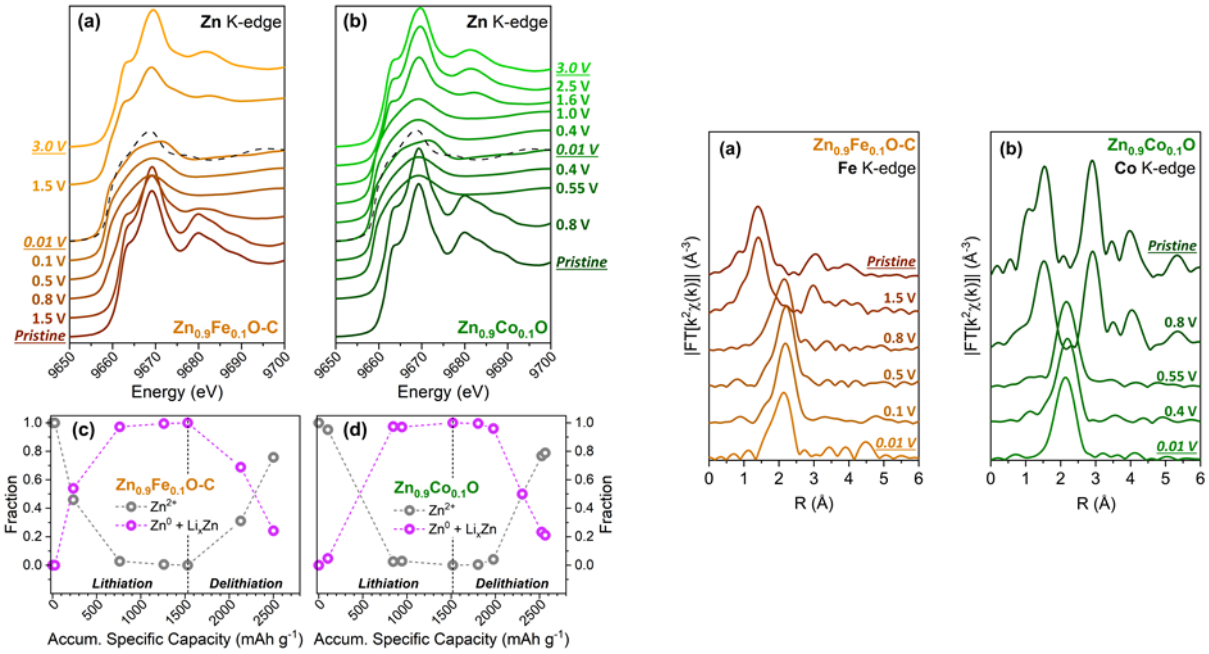

Figure *8: Left: Zn K-edge XANES spectra measured ex situ on (a) carbon-coated $Zn_{0.9}Fe_{0.1}O$ and (b) $Zn_{0.9}Co_{0.1}O$ electrodes recovered at selected potentials along the first de-/lithiation. (c,d) Fractions of oxidized Zn^{2+} and metallic zinc (Zn^0 + Li_xZn) after Li uptake and release as estimated by linear combination fitting of the Zn K-edge XANES spectra (adapted from the principal publication, with permission from Elsevier). Right: Magnitude of the Fourier transform of the Fe K-edge (a) and Co K-edge (b) k^2-weighted EXAFS signals measured ex situ on carbon-coated $Zn_{0.9}Fe_{0.1}O$ and $Zn_{0.9}Co_{0.1}O$ electrodes recovered at selected potentials along the first discharge (adapted from the principal publication, with permission from Elsevier).*

Publication: [Mater. Today Chem. 20, 100478 (2021) https://doi.org/10.1016/j.mtchem.2021.100478]

References:

[1] M. Armand et al., J. Power Sources.479, 228708 (2020)
[2] D. Bresser et al., Energy Environ. Sci. 9, 3348 (2016)
[3] G. Giuli et al., Inorg. Chem. 54, 9393 (2015); G. Giuli et al., Materials 2018, 11(1), 49
[4] C. J. Pelliccione et al., J. Electrochem. Soc. 162, A1935 (2015)

Chemical inhomogeneities at the CoFe/NiO magnetic interface

S. Laureti[1], G. Varvaro[1], D. Peddis[1,2] and F. D'Acapito[3]

[1] CNR, Istituto di Struttura della Materia, nM2-Lab, Monterotondo Scalo (Roma), 00015, Italy
[2] Università degli Studi di Genova, Dipartimento di Chimica e Chimica Industriale, nM2-Lab, Via Dodecaneso 31, Genova, 16146, Italy
[3] CNR-IOM-OGG c/o ESRF, LISA CRG, c/o ESRF BP220, F-38043 Grenoble, France

Interfacing effects arising when different magnetic phases are in close contact lead to novel magnetic physical properties and, consequently, to the development of innovative technological applications of nanostructured magnetic materials. Phenomena such as magnetic proximity effect, exchange bias (EB), exchange spring, interlayer exchange coupling and giant/tunneling magnetoresistance (GMR, TMR), have found a wide range of applications in many fields including information storage and processing, sensors, energy and biomedicine. In this systems, chemical and microstructural inhomogeneities at the interfacial region, driven by interdiffusion processes, chemical reactions, and interface roughness are inhomogeneities that may significantly affect the final properties and, if suitably controlled, may represent an additional tool to finely tune the final overall physical properties.

In this work, the change in composition across the interfacial region between two different magnetic phases induced by the deposition conditions has been studied in a Pulsed Laser Deposition (PLD) CoFe/NiO Exchange Bias bilayer. PLD is a widely used fabrication techniques for producing high-quality thin solid films (high crystalline degree and extremely smooth surfaces) offering a great degree of flexibility in varying the different process parameters. Samples were prepared by sequential deposition of NiO and CoFe on a Si (100) substrate in a PLD high vacuum chamber by keeping the substrate temperature at 250°C (S1) and 450°C (S2). A NiO layer (~15 nm thick) was grown by ablating a metallic Ni target in an oxygen pressure of 10^{-3} mbar. Then, after recovering the vacuum, a thin CoFe film of about 5 nm was deposited on top by ablating a composite Co and Fe target, at the same growth temperature.

Extended X-ray absorption fine structure (EXAFS) measurements, carried out at the LISA beamline (ESRF, Grenoble), evidenced a significant difference between the two samples. Indeed, from a qualitative point of view, the comparison between the EXAFS signals Figure 8 (left), and the Fourier Transform Figure 8 (right), acquired at the Fe-K edge, with that of a standard Fe metallic signal confirm that S1 was mainly constituted by a Fe metallic phase, with a bcc structure as expected for the CoFe alloy. On the other hand, for S2, a change in the structure is evident. In this case, the XAS signal exhibits a completely different shape closely following that of oxidized phases with a spinel structure (either maghemite or magnetite). Other possible (hydro -)oxide structures (namely, hematite or goethite) can be ruled out. As an example, in Figure 8 the comparison with the signal of a Fe_3O_4 standard phase is reported. The EXAFS result suggests that a temperature-induced redox reaction between NiO and CoFe occurred at the interfacial region, with the formation of Fe_xO_y phases.

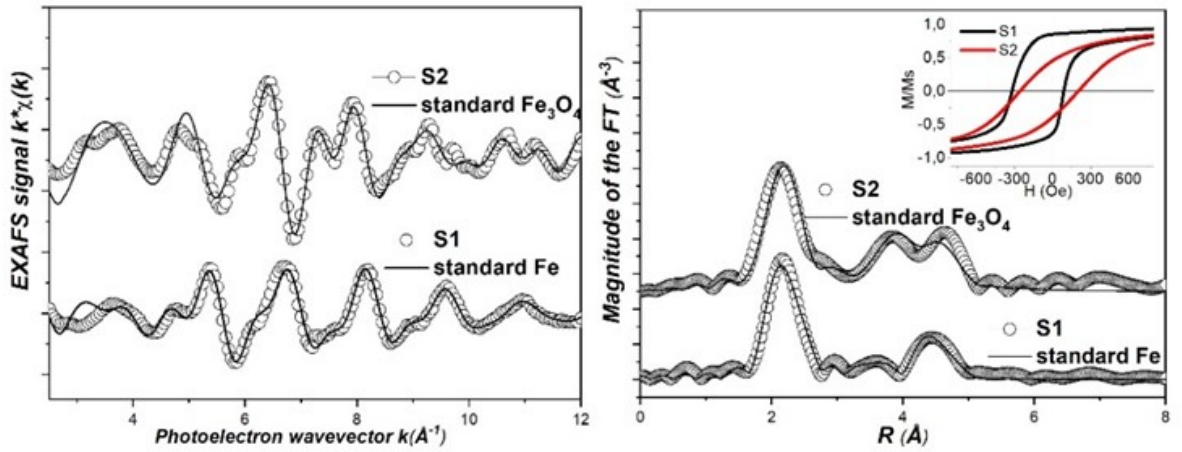

Figure 9: Comparison between EXAFS signals at the Fe-K edge (left) and corresponding Fourier transform (right); (open circles): S1 and S2 data, (solid lines): standard Fe and Fe3O4 data. XAS data extraction was carried out with the ATHENA code. Inset: Low temperature (100K) hysteresis loops after field cooling ($\mu_0 H_{cool}$ = 1 T)

From the magnetic point of view, in both samples, the Exchange Bias phenomenon evidenced by the horizontal shift of the hysteresis loop can be observed (Figure 8 right, inset). Sample S1 showed the best ratio between the exchange bias field H_{eb} and the coercive field, H_c (H_{eb} = $0.56H_c$), indicating an effective coupling between the AFM NiO phase and the FM-CoFe layer. On the other hand, sample S2 showed a smaller horizontal shift of the hysteresis loop (H_{eb} = $0.3H_c$) and significant differences in the magnetization curve. In particular, a reduced remanent magnetization Mr/Ms and an irreversible behavior (the two branches of the hysteresis loop do not merge for the whole range of applied field, not showed) suggested the occurrence of additional highly anisotropic magnetic phases taking part to the reversal process, consistently with the EXAFS study.

Publication: [S. Laureti et al. Nanotechnology, 32 (2021), 205701.]

1 Beltrami G., Di Renzo F., Parodi I., Alberti A., Guzman-Castillo M.D.L., Fajula F., Suard E., Martucci A. - Thermal activation of NH4 precursor of acidic omega zeolite: A neutron and in-situ synchrotron powder diffraction combined study Microporous and Mesoporous Materials 314, 110825-1-110825-12(2021)

2 Marmiroli M., Pagano L., Rossi R., De la Torre-Roche R., Lepore G.O., Ruotolo R., Gariani G., Bonanni V., Pollastri S., Puri A., Gianoncelli A., Aquilanti G., d'Acapito F., White J.C., Marmiroli N. - Copper oxide nanomaterial fate in plant tissue: Nanoscale impacts on repro ductive tissues Environmental Science and Technology 55, 10769-10783(2021)

3 Puri A., Lepore G., Signorato R., Scarbolo P., Di Maio G., d'Acapito F. - The LISA CRG beamline at ESRF In: "Synchrotron Radiation Science and Applications - Vol. 220", Di Cicco A. (Eds.)Giuli G. (Eds.)Trapananti A. (Eds.)(Springer, 2021) pp.57-63 In: "2019 meeting of the Italian Synchrotron Radiation Society" - Camerino, Italy - 2019--09

4 Trapananti A., Eisenmann T., Giuli G., Mueller F., Moretti A., Passerini S., Bresser D. - Iso valent vs. aliovalent transition metal doping of zinc oxide lithium-ion battery anodes — in-depth investigation by ex situ and operando X-ray absorption spectroscopy Materials Today Chemistry 20, 100478-1-100478-10(2021)

5 S Laureti, A Gerardino, F d'Acapito, D Peddis, G Varvaro The role of chemical and micro structural inhomogeneities on interface magnetism Nanotechnology 32 (2021) 205701 https://doi.org/10.1088/1361-6528/abe260

6 Fracchia M., Ghigna P., Marelli M., Scavini M., Vertova A., Rondinini S., Della Pergola R., Minguzzi A. - Molecular cluster route for the facile synthesis of a stable and active Pt nano particle catalyst. New Journal of Chemistry 45, 11292-11303(2021)

7 Pugliese, G.M.; Tortora, L.; Paris, E.; Wakita, T.; Terashima, K.; Puri, A.; Nagao, M.; Hi gashinaka, R.; Matsuda, T.D.; Aoki, Y.; Yokoya, T.; Mizokawa, T.; Saini, N.L. The Local Structure of the BiS2 Layer in RE(O,F)BiS2 Determined by In-Plane Polarized X-ray Ab sorption Measurements. Physchem 2021, 1, 250-258. https://doi.org/10.3390/ physchem1030019

8 A. Das, C Balasubramanian, P.Bhalchandra Orpe, G. Pugliese, A. Puri, A. Marcelli and N. Saini Morphological, electronic, and magnetic properties of multicomponent cobalt oxide nanoparticles synthesized by high temperature arc plasma Nanotechnology, Accepted 2021

9 Vanni M., Bellini M., Borsacchi S., Calucci L., Caporali M., Caporali S., d'Acapito F., Geppi M., Giaccherini A., Ienco A., Manca G., Mio A.M., Nicotra G., Oberhauser W., Serrano-Ruiz M., Banchelli M., Vizza F., Peruzzini M. - Interlayer coordination of Pd-Pd units in exfoliated black phosphorus Journal of the American Chemical Society 143, 10088-10098(2021)

5. Contacts

Beamline responsible:	Francesco d'Acapito dacapito@esrf.fr +33 4 7688 2426 , +33 6 8936 4302
Beamline scientists:	Michela Brunelli brunelli@esrf.fr +33 4 7688 2859
	Abdul Rehman Malik malik@iom.cnr.it +33 4 7688 2530
Local Contact:	+33 6 8838 6994
Beamline:	+33 4 7688 2085
Laboratory:	+33 4 7688 2743
Skype:	LISA_beamline@EBS
Administration:	Fabrizio La Manna lamanna@esrf.fr +33 4 7688 2962
Web page:	http://www.esrf.eu/UsersAndScience/Experiments/CRG/BM08/

Forthcoming proposals submission deadlines

ESRF quota: March 1st 2022
CERIC quota: pre-evaluation March 1st , final submission March 31st

6. Contributors to this issue

F. d'Acapito (CNR-IOM, Grenoble), R. De Donatis (CNR, Genova), S. Checchia (ESRF), S. Laureti (CNR-ISM Montelibretti), G.O. Lepore (Univ. Firenze), M. Marmiroli (Univ. Parma), A. Trapananti (Univ. Camerino), A. d'Acapito (Univ. Grenoble-Alpes), T. Baroni (Univ. Firenze).